J Mater Sci (2011) 46:4020–4025
DOI 10.1007/s10853-011-5330-1

Templated synthesis of mesoporous aluminas by *graft* copolymer and their CO_2 adsorption capacities

Harim Jeon · Sung Hoon Ahn · Jong Hak Kim · Yoon Jae Min · Ki Bong Lee

Received: 2 December 2010 / Accepted: 24 January 2011 / Published online: 10 February 2011

Abstract Mesoporous aluminas were synthesized via a sol–gel process by templating an amphiphilic *graft* copolymer, PVC–*g*–POEM, consisting of a poly(vinyl chloride) (PVC) backbone and poly(oxyethylene methacrylate) (POEM) side chains. The mesoporous structures of aluminas with large surface areas were confirmed by X-ray diffraction, transmission electron microscopy, and nitrogen adsorption/desorption analysis. Aluminas synthesized with PVC–*g*–POEM *graft* copolymer exhibited higher CO_2 adsorption capacities (0.7 mol CO_2/kg sorbent) than aluminas synthesized without *graft* copolymer (0.6 mol CO_2/kg sorbent). The adsorption capacity of alumina strongly depends on its structure and calcination temperature; amorphous (400 °C) > γ phase (800 °C) > α phase (1000 °C).

Introduction

Mesoporous materials are of special interest due to their excellent properties such as large surface areas, narrow pore-size distributions, and tunable pore sizes that are not present in the bulk state [1–4]. Alumina (Al_2O_3) has received attention in the catalysis area because of its potential applications in cracking, hydrocracking, and hydrodesulfurization of petroleum feedstocks [5–11]. The characteristics of alumina, such as large surface area, tailored pore size, high thermal stability, and capacity for modification with catalytically active species are of tremendous interest [12]. In particular, alumina is considered to be a good adsorbent for CO_2 gas [13, 14].

In general, mesoporous metal oxides are usually synthesized via sol–gel processes using ionic or non-ionic surfactants [12]. Recently, an amphiphilic *block* copolymer was utilized as a template to provide a large surface area and to control pore size [15–22]. Yuan et al. [22] synthesized ordered mesoporous γ-aluminas via a sol–gel process templated by a Pluronic series consisting of poly(ethylene oxide) (PEO) and poly(propylene oxide) (PPO) tri*block* copolymer. However, to the best of the knowledge, there have been no reports on the *graft* copolymer-directed synthesis of mesoporous alumina. *Graft* copolymers are more attractive than *block* copolymers due to their easier synthesis and low cost [23–26].

Here, we provide the first report on the synthesis of mesoporous aluminas templated by a *graft* copolymer and their CO_2 adsorption properties. An amphiphilic *graft* copolymer, PVC–*g*–POEM, consisting of poly(vinyl chloride) (PVC) backbone and poly(oxyethylene methacrylate) (POEM) side chains, was synthesized using atom transfer radical polymerization (ATRP). The structures and morphologies of the mesoporous aluminas were characterized using X-ray diffraction (XRD), transmission electron microscopy (TEM), thermogravimetric analysis (TGA) and nitrogen adsorption/desorption analysis. Equilibrium CO_2 adsorption uptake on the alumina is also reported in this article.

H. Jeon · S. H. Ahn · J. H. Kim (✉)
Department of Chemical and Biomolecular Engineering,
Yonsei University, 262 Seongsanno,
Seodaemun-gu, Seoul 120-749, South Korea
e-mail: jonghak@yonsei.ac.kr

Y. J. Min · K. B. Lee (✉)
Department of Chemical and Biological Engineering,
Korea University, Anam-dong, Seongbuk-gu,
Seoul 136-713, South Korea
e-mail: kibonglee@korea.ac.kr

Experimental procedure

Materials

Poly(vinyl chloride) (PVC, $M_w = 97{,}000$ g/mol, $M_n = 55{,}000$ g/mol); poly(oxyethylene methacrylate) (POEM, poly(ethylene glycol) methyl ether methacrylate, $M_n = 475$ g/mol); 1,1,4,7,10,10-hexamethyltriethylene tetramine (HMTETA, 99%); and copper(I) chloride (CuCl, 99%), aluminum isopropoxide, ($Al(O–Pr)_3$), and hydrochloric acid (HCl, 37 wt%) were purchased from Sigma–Aldrich.

Synthesis of the *graft* copolymer

PVC–*g*–POEM *graft* copolymer was synthesized using ATRP following a previously reported method [23, 24]. In brief, 6 g of PVC were dissolved in 50 mL of *N*-methyl-2-pyrrolidone (NMP) by stirring at 90 °C for 4 h. After cooling the solution to room temperature, 15 g of POEM, 0.1 g of CuCl, and 0.23 mL of HMTETA were added to the solution. The green mixtures were stirred until homogeneous, and purged with nitrogen for 30 min. The reaction was carried out at 90 °C for 18 h. After polymerization, the resultant mixtures were diluted with tetrahydrofuran (THF). After passing the solutions through a column with activated Al_2O_3 to remove the catalyst, the solutions were precipitated into methanol. The *grafted* copolymers were purified by dissolving in THF and reprecipitating into methanol three times. PVC–*g*–POEM *graft* copolymer with PVC:POEM = 4:6 wt ratio was obtained in a powder form and dried in a vacuum oven overnight at room temperature.

Preparation of the mesoporous alumina

First, 1 g of PVC–*g*–POEM *graft* copolymer was dissolved in 20 mL of THF and then, 1.5 mL of HCl and 2.04 g of aluminum isopropoxide (10 mmol) were added to the polymer solution at different weight ratios, i.e., PVC–*g*–POEM:$Al(O–Pr)_3$ = 1:1, 1:3, and 0:1, which are referred to as P1A1, P1A3, and P0A1, respectively. When prepared with a weight ratio of POEM:$Al(O–Pr)_3$ higher than 1:3, e.g., 1:5, the properties of the alumina ranged between 1:3 and 0:1 according to the simple mixing rule. Thus, we focused on three compositions: P1A1, P1A3, and P0A1. After vigorous stirring, the samples were put into a 50 °C oven to undergo the solvent evaporation process. After overnight aging, calcination was carried out at various temperatures, 400, 800, and 1000 °C, for 4 h with a ramping rate of 4 °C/min.

Characterization

Powder XRD analysis was carried out with a Rigaku Co. Miniflex diffractometer using CuK_α X-ray radiation at a scan speed of 3°/min. TEM images were obtained from a JEOL JEM 1010 microscope operating at 300 kV. For the TEM measurements, the samples were dispersed in alcohol and a drop of the resulting solution was then placed onto a standard copper grid. The Brunauer–Emmett–Teller (BET) surface areas, pore sizes, and pore volumes of the samples were determined from the N_2 adsorption at −196 °C using a Micromeritics Tristar 3000 system. Each sample was degassed under vacuum at 200 °C for 12 h prior to N_2 physisorption. TGA was performed to evaluate the thermal behavior of the PVC–POEM *graft* copolymer and mesoporous aluminas. TGA was carried out in a TA Instruments Q50 under N_2 gas flow with a heating rate of 10 °C/min. Equilibrium CO_2 adsorption uptake on samples was also measured via TGA. Before CO_2 adsorption experiments, samples were cleaned by flowing N_2 gas at 30 °C for 8 h. After regeneration, the change in sample weight was recorded under the condition of pure CO_2 gas flow at a pressure of ~1 atm and at a temperature of 30 °C for 10 h

Results and discussion

A hydrophilic–hydrophobic microphase-separated structure is critical for synthesizing organized mesoporous alumina. The amphiphilic PVC–*g*–POEM *graft* copolymer was used as a structure-directing agent to synthesize mesoporous aluminas via a sol–gel process using an alumina precursor, $Al(O–Pr)_3$, as represented in Scheme 1. $Al(O–Pr)_3$ is expected to be selectively incorporated into hydrophilic POEM domains where alumina crystallites are formed in situ during calcination, originating from favorable interactions between $Al(O–Pr)_3$ and POEM. Upon calcination at a temperature of 400 °C or higher, mesoporous aluminas were obtained with an average pore size of 10–27 nm.

The adsorption/desorption of nitrogen in the mesoporous aluminas was measured as shown in Fig. 1. All characterized samples corresponded to type IIb isotherms exhibiting type H3 hysteresis according to the IUPAC classification, which describes the characteristic adsorption behavior of non-rigid mesoporous solids [27]. The hysteresis indicates the presence of slit pores. The data on the BET surface area, pore size, and pore volume of P1A1, P1A3, and P0A1 are summarized in Table 1 at calcination temperatures of 400, 800, and 1000 °C. The aluminas

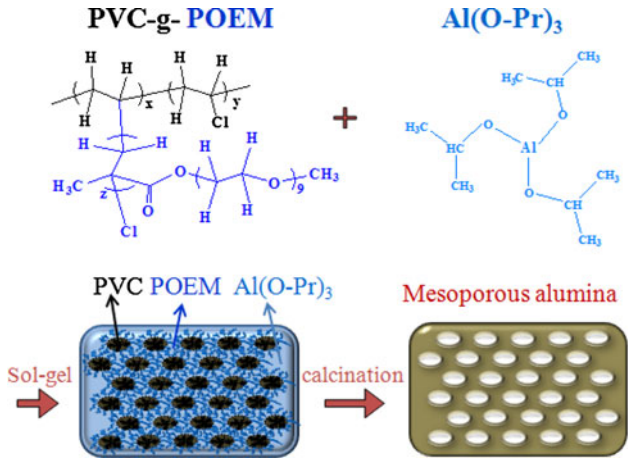

Scheme 1 Schematic illustration for the synthesis of mesoporous alumina

templated by PVC–*g*–POEM (P1A1 and P1A3) had higher surface areas and total pore volumes, and smaller average pore sizes than alumina prepared without PVC–*g*–POEM (P0A1) at all calcination temperatures. In the comparison of P1A1 and P1A3, P1A1 had a higher surface area and smaller pore size than P1A3 at the calcination temperatures of 400 and 1000 °C. However, at the calcination temperature of 800 °C, P1A3 had a higher surface area and smaller pore size. This implies that there may be different optimal ratios of PVC–*g*–POEM for surface area and porosity at different calcination temperatures. Among the tested calcination temperatures, small mesopores were best developed at 800 °C, resulting in the highest surface areas and total pore volumes. Figure 2 shows the mesopore distribution analyzed using the Barret–Joyner–Halenda method. The alumina calcined at 400 °C exhibited a narrower pore size distribution, whereas the distribution pattern at 800 °C was much broader. This suggests that alumina calcined at 400 °C is more uniformly packed together than alumina calcined at 800 and 1000 °C.

We investigated the structures and phase transitions of aluminas that were templated by the *graft* copolymer using XRD patterns, as shown in Fig. 3. The PVC–*g*–POEM *graft* copolymer was completely amorphous, exhibiting a broad peak at around 20°. The structure of alumina synthesized by $Al(O–Pr)_3$ and PVC–*g*–POEM was strongly dependent on the calcination temperature. Thermal transformation of boehmite is known to give the transition order $\gamma \rightarrow \delta \rightarrow \theta \rightarrow \alpha$ [20–22]. Pseudo-boehmite was generated as a result of the hydrolysis of $Al(O–Pr)_3$, which is transformed into transition aluminas through the same transformation sequence as boehmite. Calcination at 400 °C gave rise to the amorphous structure of alumina, which was converted to γ phase (JCPDS, card no. 29-63) after further treatment at 800 °C [22]. When the calcination temperature

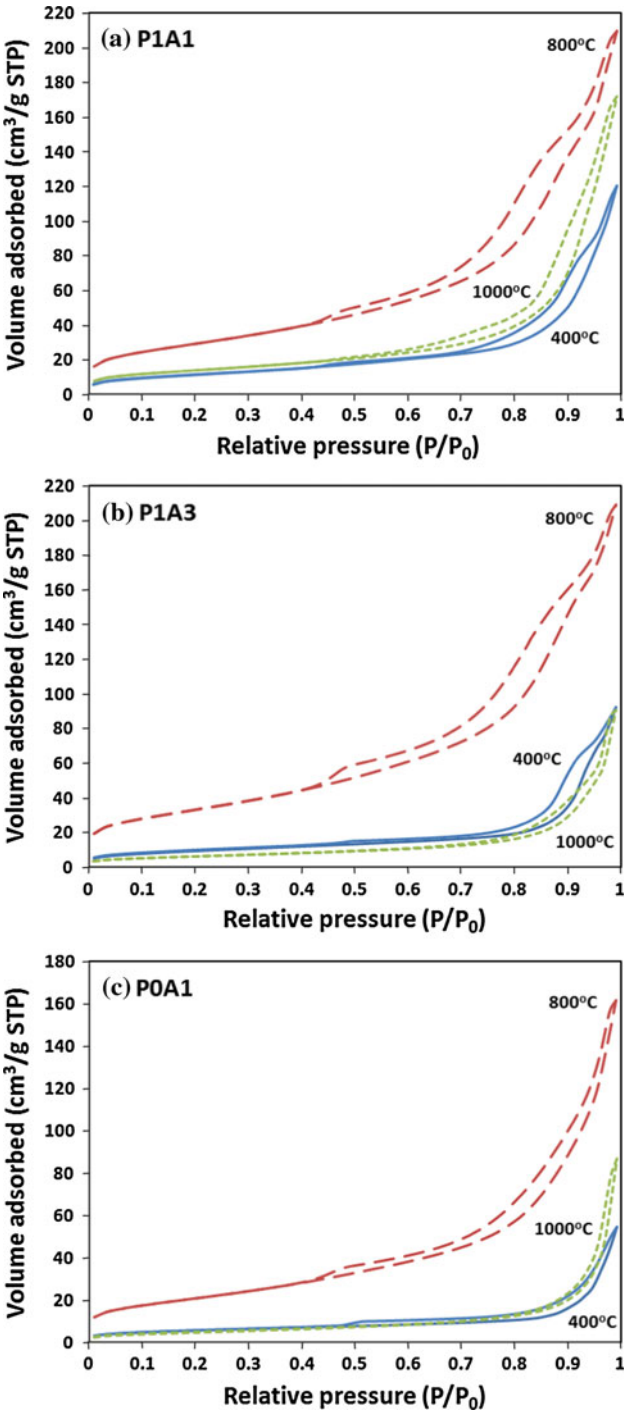

Fig. 1 Nitrogen adsorption–desorption isotherms at −196 °C for alumina after calcination at different temperatures: **a** P1A1, **b** P1A3 and **c** P0A1

was further increased to 1000 °C, several sharp peaks assigned to the α phase (JCPDS, card no. 11-0661) of alumina appeared, although the small portion of θ-phase (JCPDS, card no. 11-0517) was observed around 45.6° [20].

Table 1 Surface area and porosity of aluminas after calcination at different temperatures

	P1A1			P1A3			P0A1		
Calcination temperature (°C)	400	800	1000	400	800	1000	400	800	1000
BET surface area (m^2/g)	43.1	107.6	50.6	35.1	120.3	23.0	20.5	76.4	18.8
Average pore diameter (nm)	16.1	10.5	18.3	17.4	9.6	21.9	19.4	11.6	26.7
Total pore volume (cm^3/g)	0.183	0.325	0.263	0.139	0.319	0.140	0.082	0.247	0.133

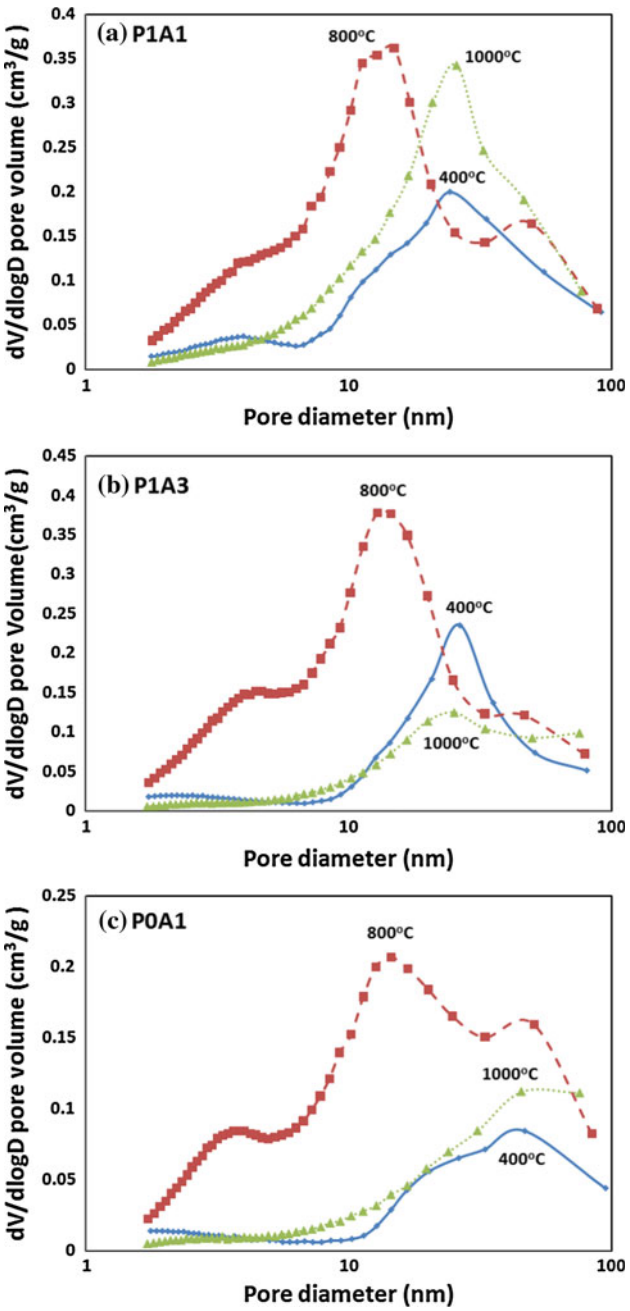

Fig. 2 Pore size distribution of alumina after calcination at different temperatures: **a** P1A1, **b** P1A3 and **c** P0A1

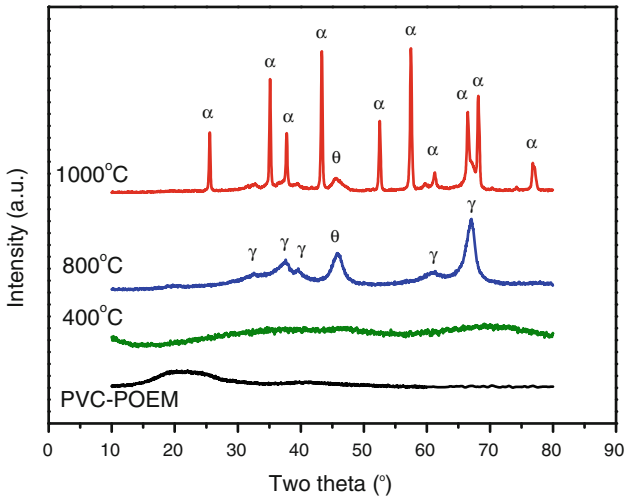

Fig. 3 XRD patterns of PVC–*g*–POEM *graft* copolymer and alumina templated by PVC–*g*–POEM after calcination at different temperatures

Evidence for mesoporous alumina was provided by TEM images, as shown in Fig. 4. The mesoporous structures were found in P1A1 and P1A3 samples that were synthesized by templating the *graft* copolymer after calcination at 400 °C, whereas a less porous structure was achieved when prepared without PVC–*g*–POEM *graft* copolymer P0A1. This indicates that PVC–*g*–POEM plays a crucial role as a structure-directing agent for generating mesoporous structures of alumina. The favorable interaction of $Al(OPr)_3$ or its hydrolysis products with POEM chains leads to preferential confinement in hydrophilic POEM chains. Through the calcination process, all of the *graft* copolymers experienced complete thermal decomposition, whereas alumina remained in the POEM domains so that the PVC domains were converted to pores and the POEM domains were taken only by alumina. For P0A1 samples without PVC–*g*–POEM, however, the precursor $Al(OPr)_3$ was unable to convert to porous alumina, leading to a dense and packed alumina structure. Upon calcination at 1000 °C, the resulting alumina segments were angulated and rougher, indicating an increase in crystallinity (Fig. 4d).

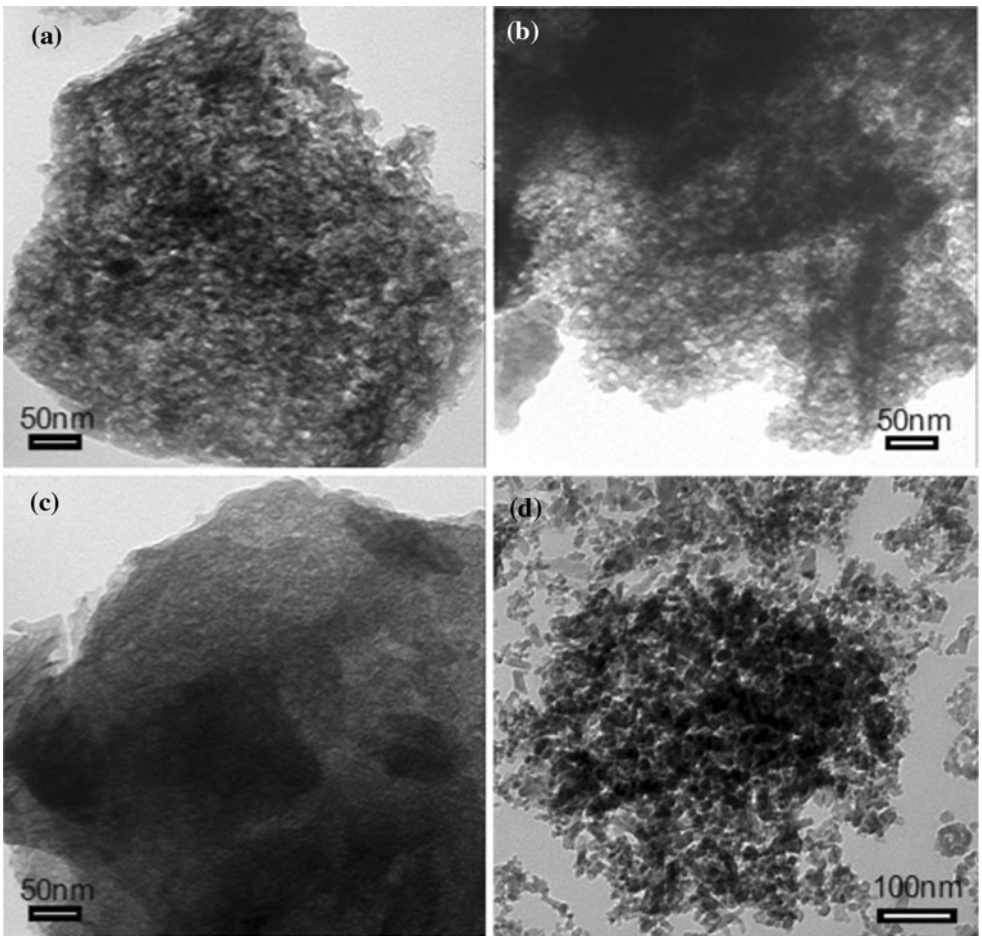

Fig. 4 TEM images of alumina: **a** P1A1 after calcination at 400 °C, **b** P1A3 after calcination at 400 °C, **c** P0A1 after calcination at 400 °C, **d** P1A1 after calcination at 1000 °C

The TGA results for PVC–POEM *graft* copolymer and P1A1 aluminas calcined at different temperatures are shown in Fig. 5. The PVC–POEM *graft* copolymers were thermally decomposed at temperatures between 240 and 550 °C. The alumina samples calcined at 800 or 1000 °C did not show significant weight loss. The alumina sample calcined at 400 °C showed about 20% weight loss until 600 °C. Some portion of the weight loss could be due to PVC–POEM *graft* copolymer remaining after calcination. However, the amount of remaining copolymer is expected to be small, because the weight loss between 240 and 550 °C is less than 6%. The major weight loss before 240 °C is probably the result of the removal of impurities such as water vapor and CO_2.

Figure 6 compares equilibrium CO_2 adsorption uptakes on P1A1, P1A3, and P0A1 after calcination at 400, 800, and 1000 °C. In all three samples, the highest equilibrium CO_2 adsorption uptake was obtained at the calcination temperature of 400 °C, and the equilibrium CO_2 adsorption uptake decreased with increasing calcination temperature. As calcination temperature increased, the alumina phase changed

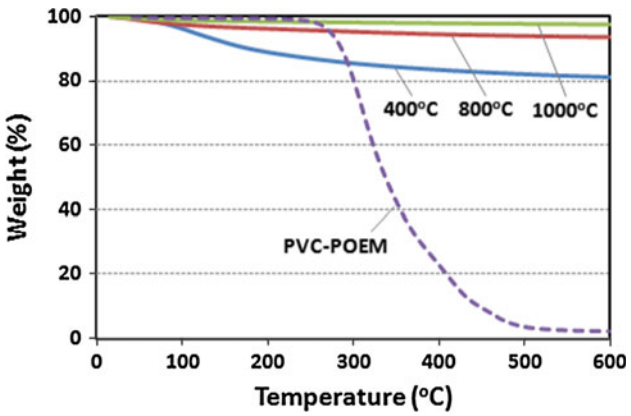

Fig. 5 TGA curves for PVC–POEM *graft* copolymer and P1A1 aluminas after calcination at different temperatures

in the order of $\gamma \rightarrow \delta \rightarrow \theta \rightarrow \alpha$ and became chemically more inert, resulting in reduced CO_2 adsorption uptake. Compared to P0A1, the equilibrium CO_2 adsorption uptake was increased by 10–50% in P1A1 and P1A3. The enhancement of CO_2 adsorption on the template-synthesized

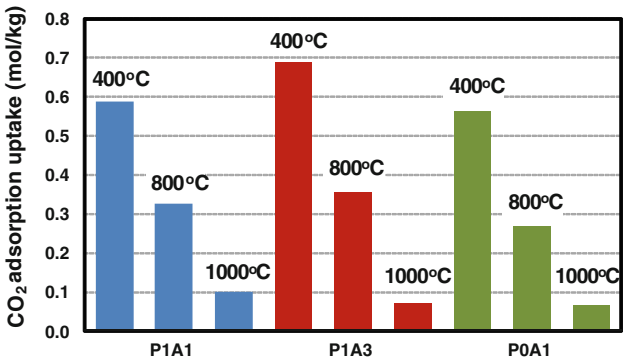

Fig. 6 Equilibrium CO_2 adsorption uptake on aluminas after calcination at different temperatures

aluminas resulted from increased surface areas that were favorable for adsorption. The CO_2 adsorption uptake of template-synthesized aluminas calcined at 400 °C is comparable with previous results reported in the literature that ranged from 0.4 to 0.9 [14, 28]. The CO_2 adsorption uptake of the template-synthesized aluminas is expected to be improved further by optimizing the preparation method.

Conclusions

This study demonstrates the use of the ATRP process to synthesize an amphiphilic PVC–*g*–POEM *graft* copolymer that was then effectively used as a template for the in situ growth of mesoporous alumina via a sol–gel process. Nitrogen adsorption/desorption analysis revealed that both the surface area and total volume of the alumina increased while the pore diameter decreased upon the utilization of the *graft* copolymer as a template. The amorphous PVC–*g*–POEM *graft* copolymer was completely amorphous, exhibiting a broad peak at around 20°, as confirmed by XRD analysis. The alumina was in an amorphous state after thermal treatment at 400 °C, which converted to γ phase at 800 °C and α phase at 1000 °C. The equilibrium CO_2 adsorption uptake on the alumina synthesized by templating PVC–*g*–POEM was always higher than that synthesized without templating, following the order of: amorphous (400 °C) > γ phase (800 °C) > α phase (1000 °C).

Acknowledgements This study was supported by a National Research Foundation (NRF) grant funded by the Korean government (MEST) through the Active Polymer Center for Pattern Integration (R11-2007-050-00000-0) and the Korea Center for Artificial Photosynthesis (KCAP) at Sogang University (NRF-2009-C1AAA001-2009-0093879). This study was also supported by the Ministry of Knowledge Economy through the Manpower Development Program for Energy.

References

1. Zubizarreta L, Arenillas A, Pis JJ, Pirard JP, Job N (2009) J Mater Sci 44:6583. doi:10.1007/s10853-009-3918-5
2. Mirzaeian M, Hall PJ (2009) J Mater Sci 44:2705. doi:10.1007/s10853-009-3355-5
3. Tang J, Wu Y, McFarland EW, Stucky GD (2004) Chem Commun 2004:1670
4. Nedelcu M, Guldin S, Orilall MC, Lee J, Hüttner S, Crossland EJW, Warren SC, Ducati C, Laity PR, Eder D, Wiesner U, Steiner U, Snaith HJ (2010) J Mater Chem 20:1261
5. Shojaie-Bahaabad M, Taheri-Nassaj E (2008) Mater Lett 62:3364
6. Kritikaki A, Tsetsekou A (2009) J Eur Ceram Soc 29:1603
7. Yao N, Xiong GX, Zhang YH, He MY, Yang WS (2001) Catal Today 68:97
8. Teng F, Wang JW, Tian ZJ, Wang ZM, Xiong GX, Xu ZS, Xu YP, Lin LW (2005) Mat Sci Eng B 116:215
9. Thiruchitrambalam M, Palkar VR, Gopinathan V (2004) Mater Lett 58:3063
10. Ono S, Masuo Y (2004) J Mater Sci 39:4367. doi:10.1023/B:JMSC.0000033428.62412.fe
11. He J, Liu W, Zhu LH, Huang QW (2005) J Mater Sci 40:3259. doi:10.1007/s10853-005-2696-y
12. Márquez-Alvarez C, Zilková N, Pérez-Pariente J, Cejka J (2008) Catal Rev 50:222
13. Mao C-F, Vannice MA (1994) Appl Catal A 111:151
14. Yong Z, Mata V, Rodrigues AE (2000) J Chem Eng Data 45:1093
15. Zukalova M, Zukal A, Kavan L, Nazeeruddin MK, Liska P, Gratzel M (2005) Nano Lett 5:1789
16. Cheng YJ, Gutmann JS (2006) J Am Chem Soc 128:4658
17. Wan Lj, Fu HG, Shi KY, Tian XQ (2008) Mater Lett 62:1525
18. Chen L, Yao B, Cao B, Fan K (2007) J Phys Chem C 111:11849
19. Yun HS, Miyazawa K, Zhou H, Honma I, Kuwabara M (2001) Adv Mater 13:1377
20. Tahmasebpour M, Babaluo AA, Shafiei S, Pipelzadeh E (2009) Powder Technol 191:91
21. Zhang ZR, Hicks RW, Pauly TR, Pinnavaia TJ (2002) J Am Chem Soc 124:1592
22. Yuan Q, Yin AX, Luo C, Sun LD, Zhang YW, Duan WT, Liu HC, Yan CH (2008) J Am Chem Soc 130:3465
23. Ahn SH, Koh JH, Seo JA, Kim JH (2010) Chem Commun 46:1935
24. Lee KJ, Park JT, Goh JH, Kim JH (2008) J Polym Sci A 46:3911
25. Kim YW, Park JT, Koh JH, Roh DK, Kim JH (2008) J Membr Sci 325:319
26. Nasef MM, Hegazy EA (2004) Prog Polym Sci 29:499
27. Rouquerol F, Rouquerol J, Sing K (1999) Adsorption by powders and porous solids. Academic Press, London
28. Li G, Xiao P, Webley P (2009) Langmuir 25:10666